Numerical Study of the Primary Instability in a Separated Boundary Layer Transition under Elevated Free-Stream Turbulence

Mostafa Langari [a] and Zhiyin Yang [b]

Department of Engineering and Design, Sussex University, Brighton BN1 9RH, U.K.

Abstract

Numerical studies of laminar-to-turbulent transition in a separation bubble subjected to two free-stream turbulence levels (FST) have been performed using Large-Eddy Simulation (LES). Separation of the laminar boundary layer occurs at a curvature change over a plate with a semi-circular leading edge at Re = 3450 based on the plate thickness and the uniform inlet velocity. A numerical trip is used to produce the targeted free-stream turbulence levels and the decay of free-stream turbulence is also well predicted. A dynamic Sub-grid-scale (SGS) model is employed in the current study and a good agreement has been obtained between the LES results and the experimental data. Detailed analysis of the LES data has been carried out to investigate the primary instability mechanism. The flow visualisations and spectral analysis of the separated shear layer reveal that the 2D Kelvin-Helmholtz instability mode, well known to occur at low FST levels, is bypassed at higher levels leading to earlier breakdown to turbulence.

I. INTRODUCTION

Laminar-to-turbulent transition in separated flows is a common feature in many practical engineering flows. Transition plays a key role in aerodynamics and heat transfer characteristics of many such flow systems. The location of transition onset, transition process, and the extent of region within which transition takes place are crucial in

[a] Electronic mail: m.langari@sussex.ac.uk

[b] Corresponding author: Zhiyin.Yang@sussex.ac.uk

engineering design and performance prediction applications. Transition is a complex process whereby certain frequencies in the disturbance signal are selectively amplified by the unstable shear layer flow, behaving differently from case to case according to the distributions of energy in the disturbance. Transition process starts with flow instabilities and is strongly affected by a number of factors such as free-stream turbulence level, streamwise pressure gradient and wall roughness etc.

Several numerical studies have considered separated boundary layer transition under vanishingly low environmental disturbances (Spalart & Strelets [1], Yang & Voke [2], Abdalla & Yang [3-4], McAuliffe & Yaras [5]). Direct Numerical Simulation (DNS) of Spalart & Strelets [1] for a bubble induced by an adverse pressure gradient over a flat plate under very low incoming disturbances revealed a wavering behaviour of the separated shear layer gradually moving away from the wall with formation of Kelvin-Helmholtz (KH) vortices. The KH vortices then rapidly developed into 3D structures and a sudden transition was reported. LES of Yang & Voke [2] for a separated shear layer on a flat plate with a semi-circular leading edge and LES of Abdalla & Yang [3] on a flat plate with a sharp leading edge proved vigorously for both cases that the free shear layer in the bubble is inviscidly unstable via the KH mechanism. Similar mechanism was reported by McAuliffe & Yaras [5] who performed DNS of a separation bubble on a flat plate in adverse pressure gradient with low incoming disturbances. Many experiments have been carried out to study separated boundary layer transition at low free-stream turbulence level. Burgmann, Dannemann and Schroder [6] studied a transitional separation bubble on the upper surface of an SD7003 airfoil using time-resolved and volumetric PIV measurements. It was shown from their measurements that the temporal dynamics of the vortex roll-up is initialized by the Kelvin–Helmholtz (KH) instability. McAuliffe & Yaras [7] carried out a through experimental study on the nature of transition in a separation bubble and manipulations of the resultant

breakdown to turbulence through passive means of control. Their results confirmed that the Kelvin-Helmholtz instability is the dominant transition mechanism for all conditions. Satta *et al*. [8] performed experimental studies of the transition and separation processes occurring along the suction side boundary layer of a high-lift low pressure turbine profile under both steady and unsteady inflow conditions. Under steady inflow condition, their results show that the beginning of boundary layer transition occurs in correspondence of the separated shear layer, along the line of inflection points in the velocity profiles, where the velocity fluctuations are larger due to the shear layer instability taking place through the Kelvin-Helmholtz mechanism. Dahnert, Lyko and Peitsch [9] drew conclusion that the instability involved in the transition process of a separation bubble with low Reynolds number, low free-stream turbulence, and steady main flow conditions is the inviscid Kelvin-Helmholtz instability mode based on their detailed experimental work.

Under increased free-stream disturbances transition process and the flow structures involved are known to be remarkably different. FST results in an earlier transition to turbulence and hence usually a shorter separation bubble (Hillier & Cherry [10], Kalter & Fernholz [11], Yang & Abdalla [4], Castro & Haque [12]). McAuliffe & Yaras [5] studied the effect of elevated FST (1.45% at separation) on a laminar separated boundary layer due to an adverse pressure gradient over a flat plate. The KH instability observed in their low-disturbance case (0.1% FST at separation) was bypassed at the higher FST where streamwise streaks appeared upstream of separation in the laminar boundary layer leading to production of turbulent spots in the separated shear layer. Bypass mode has also been observed in a few experiments on separation bubbles (Volino & Bohl [13], Volino [14]), however in all cases separation took place after relatively long streamwise development of the attached boundary layer which had a big impact on the transition in the following separated free shear layer. In cases where separation is due to the leading edge geometry and the boundary layer separates

immediately or very shortly after the leading edge, transition may be different. Yang & Abdalla [4,15] investigated the effect of 2% FST at the sharp leading edge of a flat plate and observed that transition process started earlier with a reduction of 14% in the mean bubble length compared against the very low FST case of Abdalla & Yang [3]. Nevertheless, 2D KH rolls were still observable and the primary instability was shown to be the same (the KH mechanism) as in the low FST case. However, it is quite possible if the levels of FST are increased much further than 2% transition process in a separated boundary layer with the separation point fixed due to the leading edge geometry may take a quite different route, i.e., KH instability stage may be bypassed, similar to the so called "bypass transition" in attached boundary layer flows without the intervention of viscous Tollmien–Schlichting (TS) instability waves, i.e., TS instability is bypassed and the transition is more rapid.

This paper will address this particular issue and investigate the primary instability of a separated boundary layer under 5.6% FST on a flat plate with a semi-circular leading edge, the so called ERCOFTAC (European Research Community on Flow, Turbulence and Combustion) T3L test cases where experimental data are available for mean turbulent quantities.

II. FLOW CONFIGURATION

A separated boundary layer transition on a flat plate with a semi-circular leading edge (Figure 1) of radius R = 5 mm is examined under different free-stream velocity and turbulence intensities. Figure 1 shows the sketch of the experiment with the location marked where free-stream turbulence level is measured. Four different turbulence grid configurations at three inlet velocities 2.5, 5.0, and 10.0m/s were used resulting in FST levels from 0.2% (no turbulence grid), 0.65%, 2.3%, and 5.6%. Although limited in providing near wall data, these experimental data have been the benchmark for assessing various numerical models of

transitional flow, due to the simple geometric configuration and hence possibility of accurate measurements. Two cases with different FST levels at the leading edge have been simulated in the current study at Re = 3450 based on the plate thickness (0.01m) and the uniform inlet velocity (U_0 = 5.0m/s), one with FST levels nearly zero (0.2%) denoted as Low-Turbulence-Level case (LTL-case) and one with FST = 5.6% denoted as Enhanced-Turbulence-Level case (ETL-case).

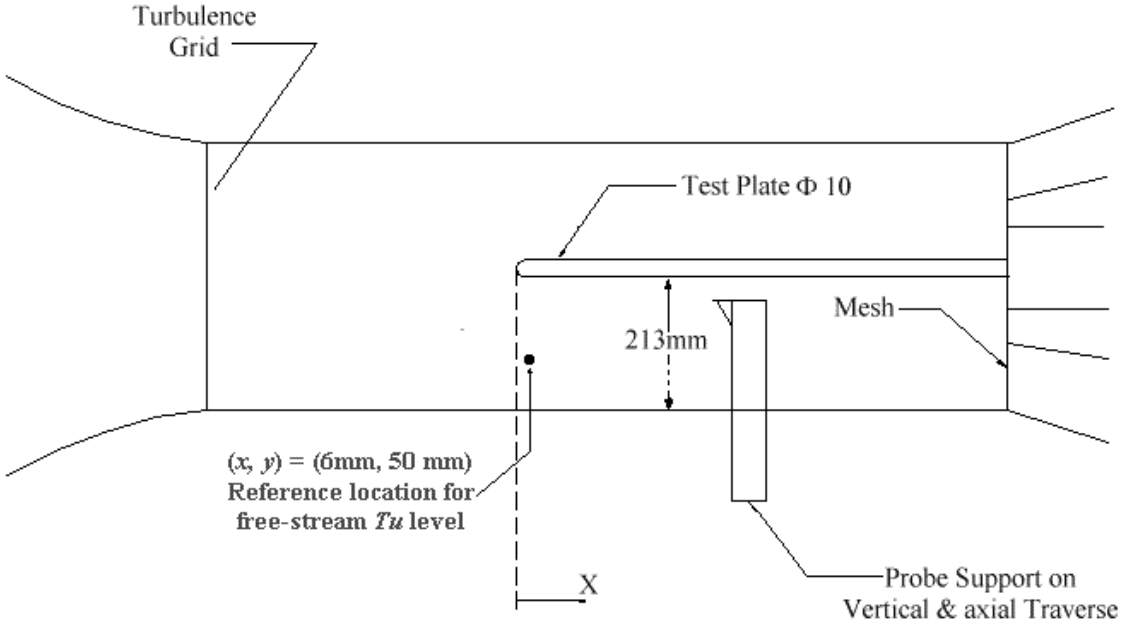

FIG. 1. Sketch of the experimental setup

The flow geometry and computational grid are shown in Figure 2. LES domain extends 12D upstream and 16D downstream from the plate leading edge, 8.5D away from the plate in the free stream, and 8D in the spanwise direction (D = 10mm is the plate thickness, and co-ordinate origin located at the stagnation point). Using the multi-block functionality, the domain is divided into 14 blocks with a grid resolution of (n_x, n_y, n_z) = (310, 140, 64) for the outer region and a refined C-grid (420, 60, 64) around the plate covering the close wall region and the free shear layer region of the separation bubble, a total of 4.39 million mesh points. Based on the friction velocity at x/D=10, which is far downstream from the separation

bubble and well within the reattached turbulent boundary layer, y^+ of the nearest cell to the wall is about 0.4, the streamwise mesh sizes vary from $\Delta x^+ = 3$ to 55 and Δz^+ is 24.

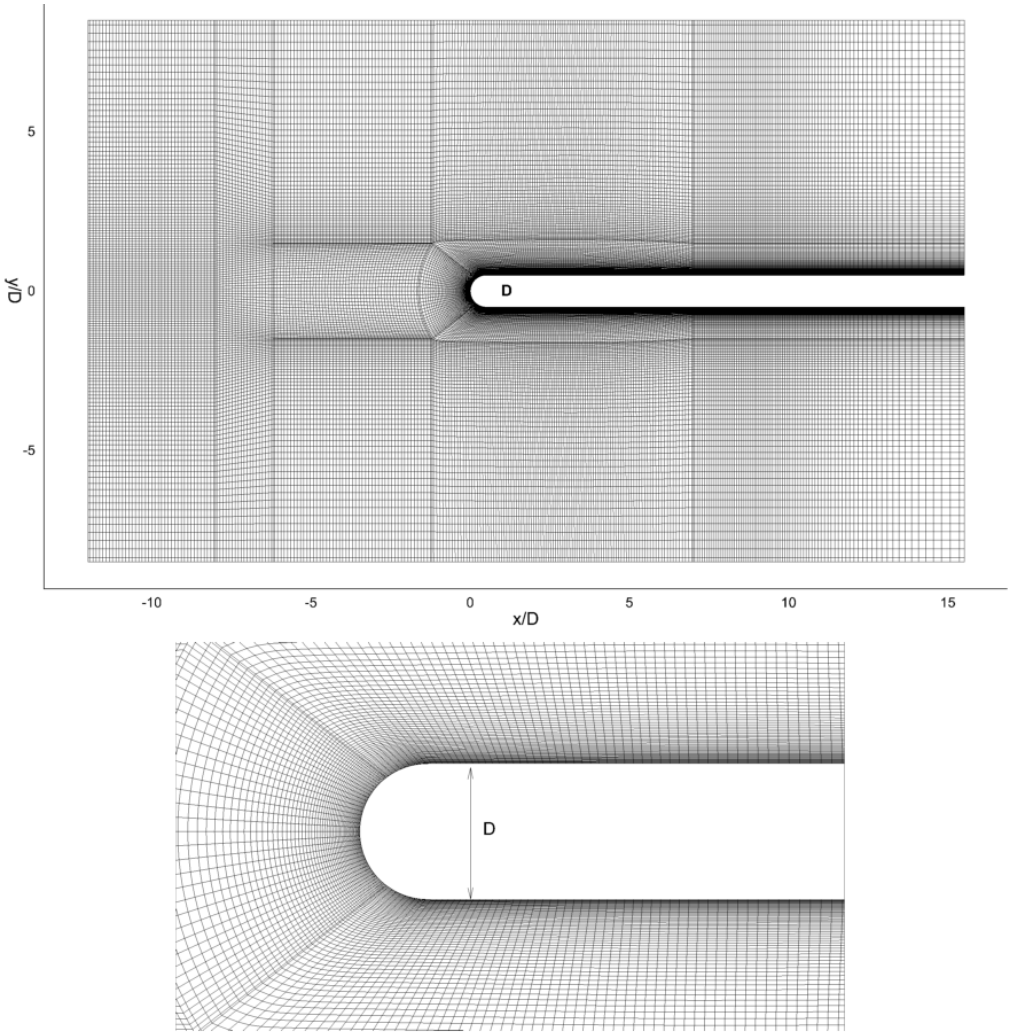

FIG. 2. Computational domain and mesh

The inflow velocity U_0 is constant aligned with the plate and applied at x = -12D upstream. For LTL-case to mimic the low turbulence level (< 0.2%) of the experiment, small random disturbances (white noise) are imposed on the mean velocity components at the inflow as $(u', v', w') = U_0.A\ (r_1, r_2, r_3)$, where A is the disturbance level (0.02 in current study) and r_1, r_2, r_3 are components of a 3D random vector. For ETL-case, a numerical trip is applied at x = -10D upstream, where at each computational time step the solution is perturbed

in a plane parallel to the inflow in the same manner as described above, but additionally, 1/2 of the disturbance magnitude is imposed upstream I-1 and downstream I+1 of tripping plane and to adjacent points J ± 1 and K ± 1, where I, J, and K are the grid indices in x, y and z directions. Also 1/4 of the disturbance magnitude is imposed at next level points i.e. J ± 2 and K ± 2, increasing the coherence of disturbance. The disturbance level (A = 0.7) was adjusted so that the experimental turbulence intensity of Tu = 5.6% at the leading edge is achieved. A convective outlet boundary condition is used ensuring the convection of the flow through the outlet plane. Periodic boundary condition is used in the spanwise direction. At lateral boundaries free-slip condition is applied and no-slip wall condition is applied at the plate surface.

III. COMPUTATIONAL DETAILS

An in-house LES code is used; details of the mathematical formulation and numerical methods can be found in Pokora *et al.* [16]. LES equations are derived by implicit spatial filtering of Navier-Stokes equations. A dynamic SGS model based on Germano *et al.* [17] and Lilly [18] is implemented where the model coefficient C is obtained as described in Yang & Voke [2]. Co-located arrangement of flow variables on a curvilinear coordinate system is used with the standard Rhie-Chow pressure smoothing. The 2nd order central differencing scheme is used for spatial discretisation. For time discretization, a single stage backwards Euler scheme has been found to be computationally more efficient to use. This is justified by small time step used in the present LES ($\Delta t = 5.0\times10^{-06}$ sec) and hence no noticeable impact on the accuracy.

The simulation ran for 10 flow-through times to allow the flow to become well established and reach a statistically stationary state. The averaged results were gathered over

further 50 flow-through times with samples taken every 10 steps and averaged over spanwise direction too.

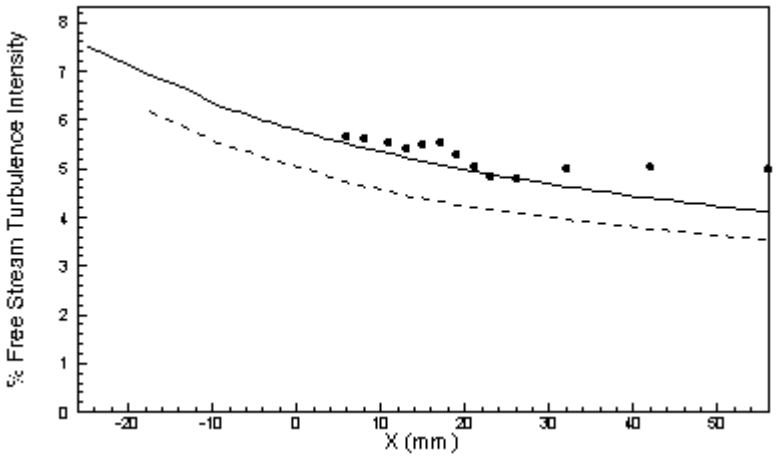

FIG. 3. Decay of free-stream turbulence intensity for ETL-case (5.6% at leading edge), Soling line: *y*/D =4.0; Dashed line: *y*/D=1.5

IV. RESULTS

For the ETL-case, it is crucial to generate the targeted FST level which decays at the right rate. Figure 3 shows the decay rate of FST intensity and it can be seen clearly that a reasonably good agreement has been obtained between the LES prediction and the experimental data at *y*/D = 4.0 although the LES results show a continuous decay further downstream while the measured FST seems to be constant, not decaying anymore which is unusual. The difference was initially thought to be due to the fact that further downstream experimental data are available only at a lower vertical location of *y*/D = 1.5, but plotting the LES results at the same vertical location of *y*/D = 1.5 (dashed line) confirms that this is not the case as the LES results still show a continuous decay which seems to be logical. Nevertheless at the leading edge the LES results match the targeted experimental FST level of 5.6% very well, indicating that the numerical trip applied upstream was a successful technique for generating the required FST at the leading edge.

A. Mean variables

For the LTL-case, Figures 4, 5 show the simulated mean streamwise velocity and rms of fluctuations, respectively. Mean and rms values are normalized by the inlet velocity (U_0). Wall-normal direction is normalized by the mean reattachment length *l*. A good agreement has been obtained between the current predicted profiles with the experimental data and LES of Yang & Voke [2] at seven streamwise stations. There is hardly any difference between the current LES results and the LES results of Yang and Voke (2001) in terms of the mean velocity predictions while for the rms the present LES results have a slightly better overall agreement with the experimental data, especially at the 5th location where the current predictions follow the experimental data much more closely although at the 6th location the peak value is better predicted by Yang and Voke [2]. However, at the last location further away from the wall the current predictions are much better than the results by Yang and Voke [2]. It is also interesting to note that the present rms results show double peaks inside the separation bubble at the 2nd and 3rd locations, especially apparent at the 3rd location whereas the LES results of Yang and Voke [2] only show one peak. Unfortunately the measurements could not be done very close to the wall inside the bubble so that the first peak near the wall cannot be confirmed by the experimental data. The measured mean bubble length (2.75D) is slightly over-predicted by about 8.9% in the current study while it is under-predicted by about 6% in the previous study on a staggered grid by Yang and Voke [2].

From the above comparison and discussion it is evident that the accuracy of predictions using the co-located grid is as good as that using the staggered grid, or even slightly better for the separated boundary layer transition over a flat plate with a semi-circular leading edge. This is consistent with the previous studies for steady flow calculations (Miller and Schmidt [19]; Peric, Kessler and Scheuerer [20]; Melaaen [21]) and unsteady flow calculations by Zang, Street and Koseff [22]. The main possible reason for the current

slightly better predictions using the co-located grid than the predictions by Yang and Voke [2] on the staggered is due to better grid resolutions in both x and y directions in important flow regions such as the near wall region, the free shear layer region in the bubble, the blend point region and the reattachment point region. It may be partly because of a larger computational domain being used so that the inflow and outflow boundaries are further away and hence have smaller influence on the results.

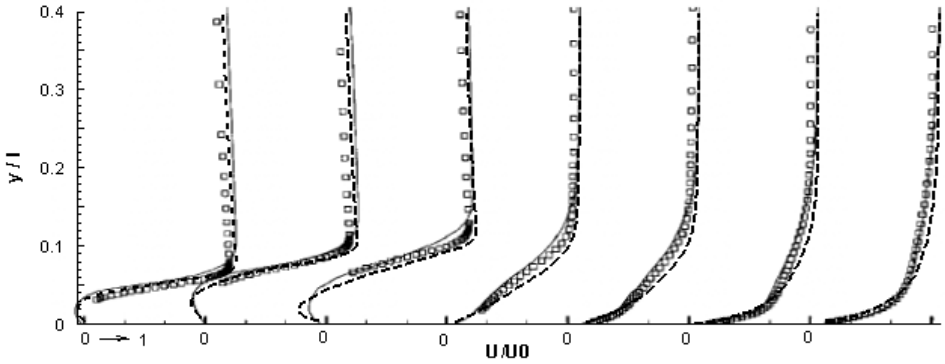

FIG. 4. Mean streamwise velocity at seven streamwise stations (LTL-case), Left to right: *x/l* = 0.22, 0.44, 0.66, 1.09, 1.27, 1.64, 2.55. Present LES (dashed), LES of Yang & Voke [2] (solid line), Exp. Data (symbols)

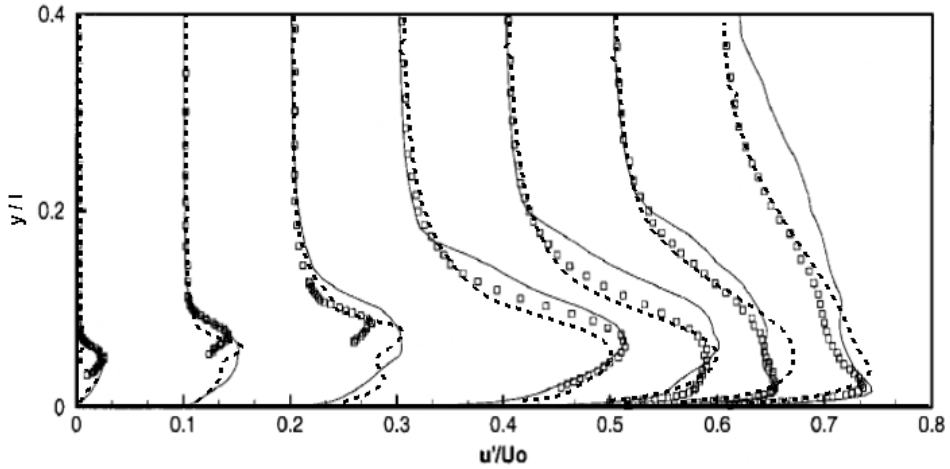

FIG. 5. rms streamwise velocity fluctuation *u′* at seven streamwise stations (LTL-case), Left to right: *x/l* = 0.22, 0.44, 0.66, 1.09, 1.27, 1.64, 2.55. Present LES (dashed), LES of Yang & Voke [2] (solid line), Exp. Data (symbols)

Figures 6, 7 present comparison between the current predicted mean streamwise velocity and rms of fluctuations with the experimental data for the ETL-case (Yang and Voke only carried out study for the LTL-case). An excellent agreement has been obtained between the predicted mean profiles and the experimental data at all streamwise locations except the last station where the mean profile is slightly over-predicted. According to the prediction there is about 40 % reduction in mean bubble size (both in length and height) for the ETL-case which is consistent with previous studies. The predicted rms of streamwise fluctuations compare very well with the experimental data in terms of both peak values and their locations. There is a slight under-prediction at two streamwise locations but overall a good agreement has been obtained. Since Δz^+ is 24 which is much bigger than the minimum Δx^+ and Δy^+, a grid refinement has been carried out in the spanwise direction (increased from 64 nodes to 100 nodes) and the peak rms values obtained with the refined mesh closer to the experimental data as shown in Figure 8.

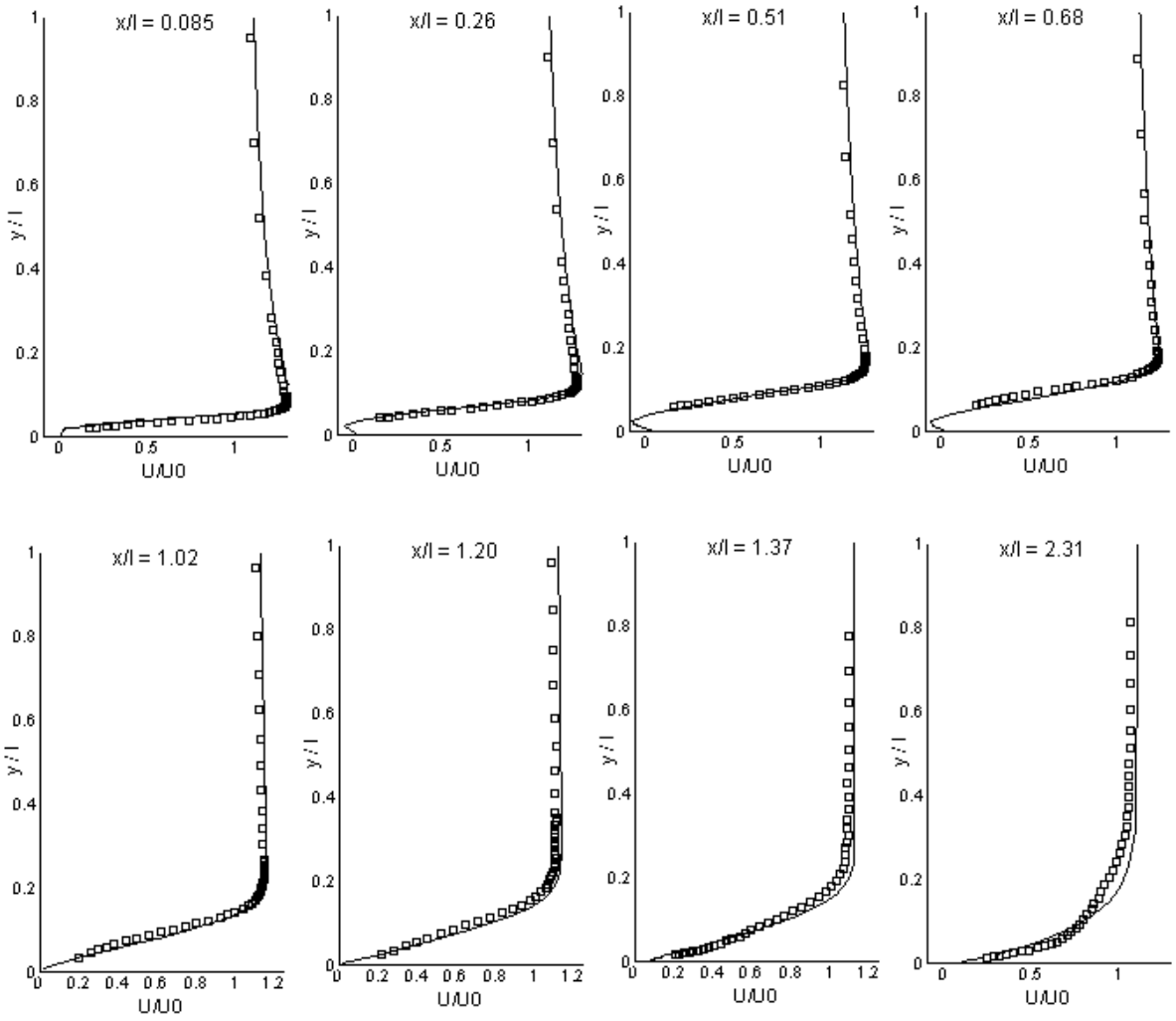

FIG. 6. Mean streamwise velocity at different streamwise stations (ETL-case), Present LES (solid lines), Exp. Data (symbols)

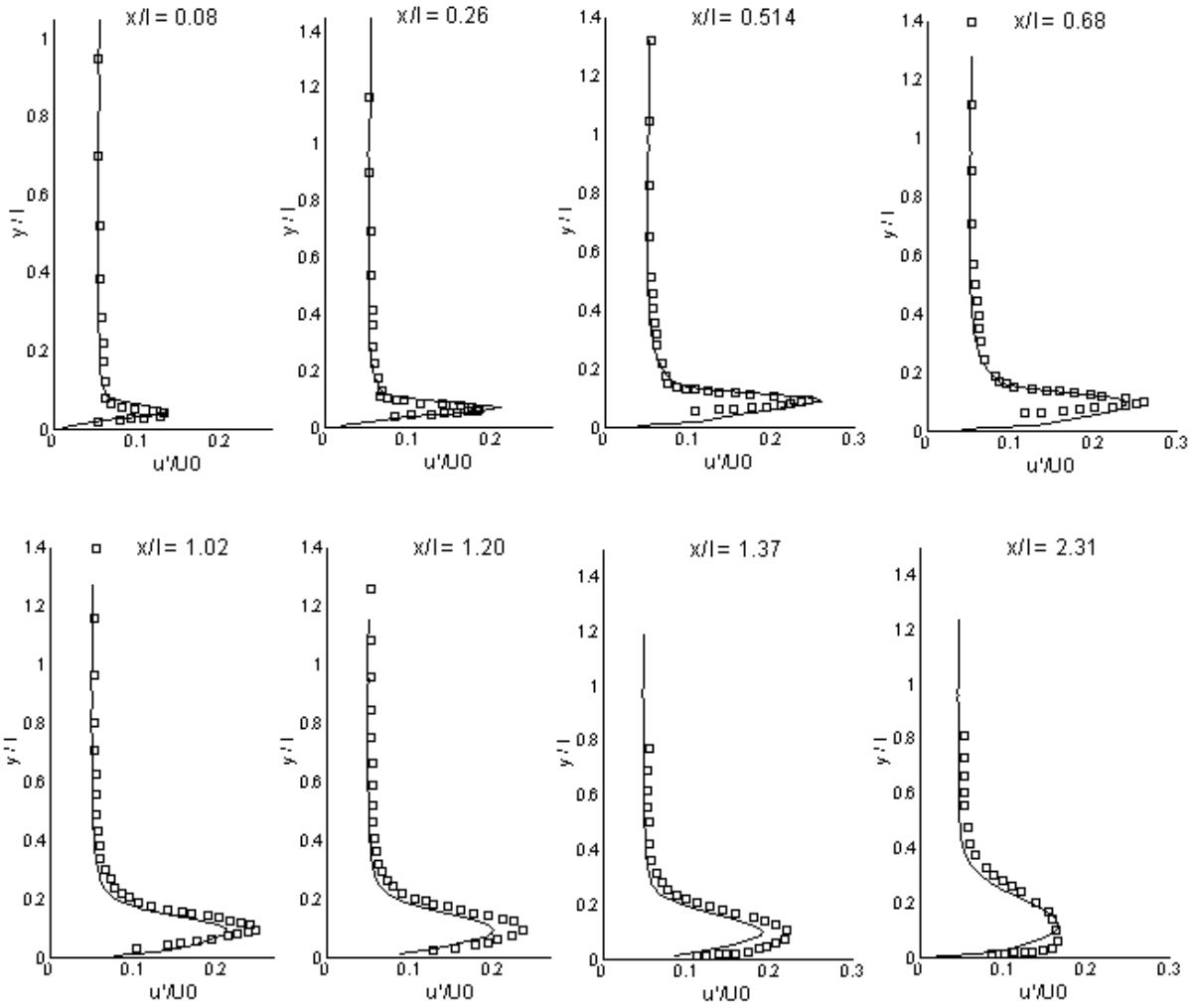

FIG. 7. rms streamwise velocity fluctuation *u'* at different streamwise stations (ETL-case), Present LES (solid lines), Exp. Data (symbols)

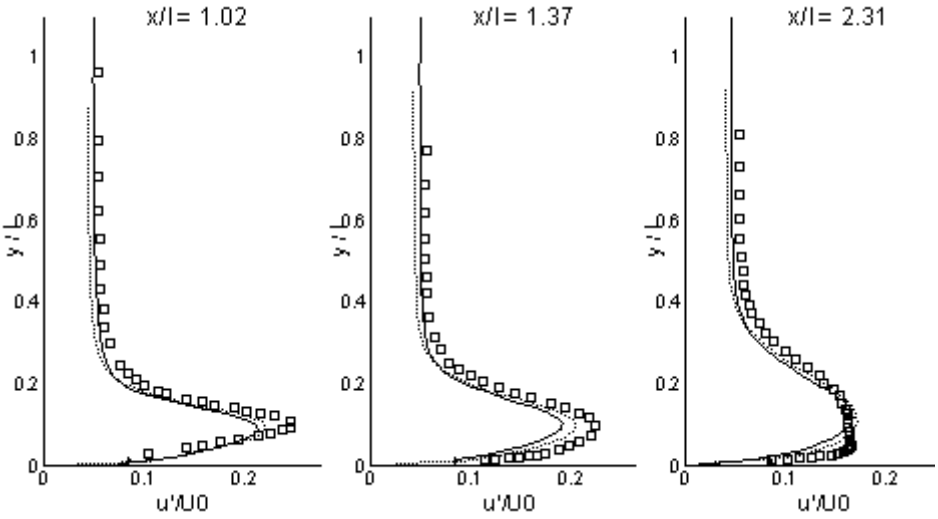

FIG. 8. rms streamwise velocity fluctuation *u'* at different streamwise stations (ETL-case), coarser grid (solid lines), refined grid (dotted lines), Exp. Data (symbols)

B. Transition process

Isosurfaces of instantaneous spanwise vorticity are presented in Figure 9 for both the LTL-case and the ETL-case at three different time, showing the transition process. The laminar boundary layer starts developing from the mean stagnation point, and then separates at the blend point due to the curvature change, leading to unstable free shear layer formed in the separation bubble. It can be seen that for the LTL-case, initially a steady free shear layer develops associated with formation of two-dimensional spanwise vortices; the free shear layer becomes unstable at about x/D = 2.1 via an inviscid instability, Kelvin-Helmholtz instability as shown in the study by Yang & Voke [2]. Any small disturbances present grow downstream causing the deformation and distortion of the initial two-dimensional spanwise vortices. Further downstream those two-dimensional vortices become more distorted/deformed, and roll up leading to the formation of streamwise vortices associated with significant three-dimensional motions, eventually breaking down at about the reattachment point and developing rapidly into a turbulent layer downstream.

For the ETL-case, as shown in Figure 9, disturbances in the free shear layer have larger amplitudes much earlier at about x/D = 0.8 due to disturbances from free-stream turbulence. Furthermore it can be seen that the flow in the attached thin boundary layer prior to separation is quite smooth, indicating that it is still laminar boundary layer but is already disturbed to some extent. Careful observation reveals that the spanwise vorticity in the ETL-case is distorted/deformed very early on and the attached thin laminar boundary layer prior to separation is not quite two-dimensional as some kind of streaky-like structures are visible. There is an increasing amount of evidence (Schlatter *et al.* [23], Watmuff *et al.* [24], Brandt & Henningson [25]) that streaky streamwise-oriented structures confined in the laminar boundary layer are the embryo for the so called "bypass" transition in attached boundary layer flows.

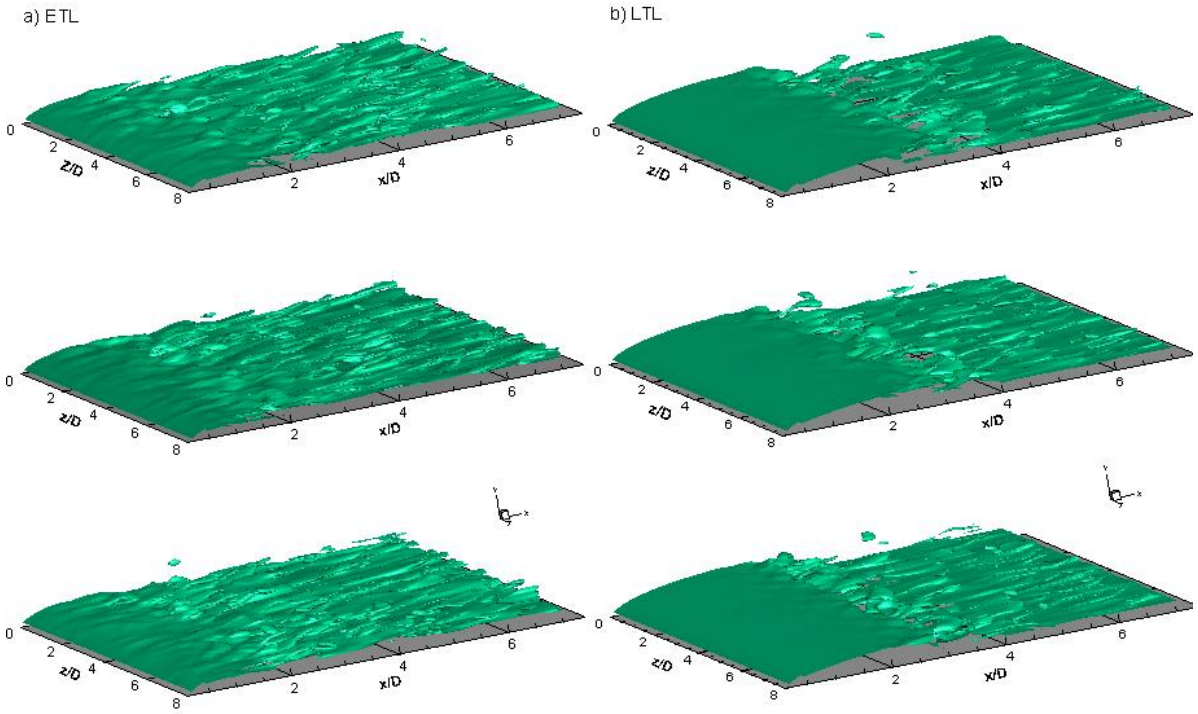

FIG. 9. Isosurfaces of instantaneous spanwise vorticity at three different time; (a) ETL-case, (b) LTL-case

To clarify what is happening in the boundary layer developing from the stagnation point to the blend point where separation occurs and further downstream, the growth of maximum turbulent kinetic energy (k_{max}, the spanwise averaged peak value of k profile along the wall normal direction in the boundary layer and free shear layer) is presented in Figure 10. It can be seen clearly that k_{max} is non-zero before separation for the ETL-case, decreasing slightly in the attached thin boundary layer since the flow accelerates along the semi-circular leading edge but starting to grow very rapidly after separation and reaching the peak in the separation bubble at about x/D = 1.1. While for the LTL-case k_{max} is zero in the attached thin boundary layer and starts to grow at about x/D = 1, well after the separation at a very low rate until at about x/D = 1.8 where k_{max} grows very rapidly at a much higher rate, reaching the peak at about x/D = 3.2. The maximum turbulence energy profiles along the plate clearly show that for the ETL-case the attached thin boundary layer is receptive to the free stream turbulence before separation, carrying a small amount of turbulent kinetic energy at separation which

grows very rapidly after the separation, leading to much earlier transition and breakdown to turbulent flow.

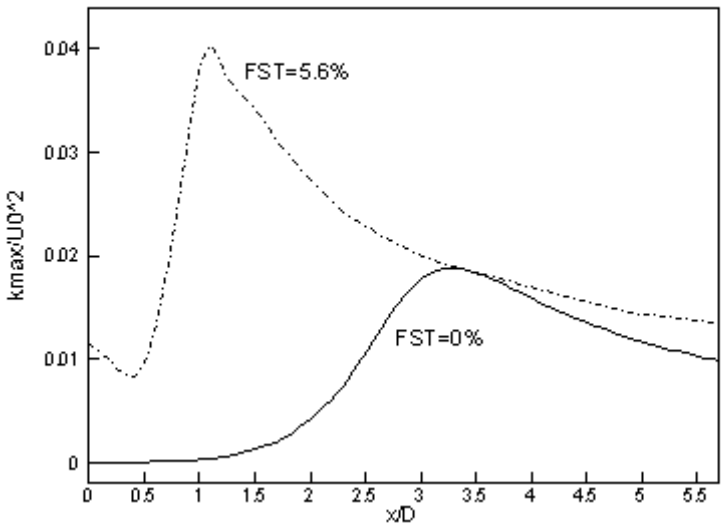

FIG. 10. Development of the maximum turbulent kinetic energy; LTL-case (solid line), ETL-case (dashed line)

The above discussion has indicated that for the ETL-case a kind of "bypass" transition may have taken place, i.e., the KH instability is bypassed. To further investigate if this is indeed the case the procedure presented by Yang & Voke [2] is followed here. For an incompressible free shear layer the criterion for the KH instability to occur is 0< Kh <1.2788 (Chandrasekhar [26]); where K is the wave number and h is the shear layer thickness. Figure 11 shows the streamwise velocity spectra for the LTL-case. The spectral analysis for other components of velocity and pressure over a wide region of separated shear layer returns very similar frequency content. A clear peak region is observed with the average characteristic frequency $f = 0.86U_0/l$ (l is the mean bubble length) which is close to the value previously predicted by Yang & Voke [2] and the measured characteristic frequency. The Kh value in the current study is also very close to that of Yang & Voke [2], confirming that the instability mechanism at work is through the KH instability mode. However, for the ETL-case, only a mild peak region could be observed at about x/l = 0.085 and y/l = 0.023 with the average

characteristic frequency $f = 1.56U_0/l$ as shown in Figure 12. The wave speed c is equal to the velocity at the critical layer, i.e. the streamwise velocity at the inflection point (x/l = 0.085, y/l = 0.026), which is $0.59U_0$ so that the wave number $K = 2\pi f/c = 16.61/l$. The shear layer thickness at this streamwise location (x/l = 0.085) is roughly about $h = 0.089l$ and hence Kh = 1.48 which does not satisfy the KH instability criterion ($0 < kh < 1.2788$). Therefore the primary KH instability observed under low free-stream turbulence is bypassed at the high free-stream turbulence level of 5.6% examined in the current study.

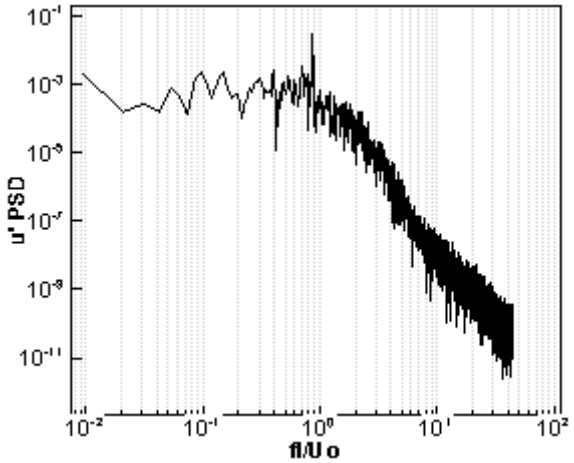

FIG. 11. Power spectrum of streamwise velocity fluctuation *u'* at *x/l* = 0.9 and *y/l* = 0.02 (LTL-case)

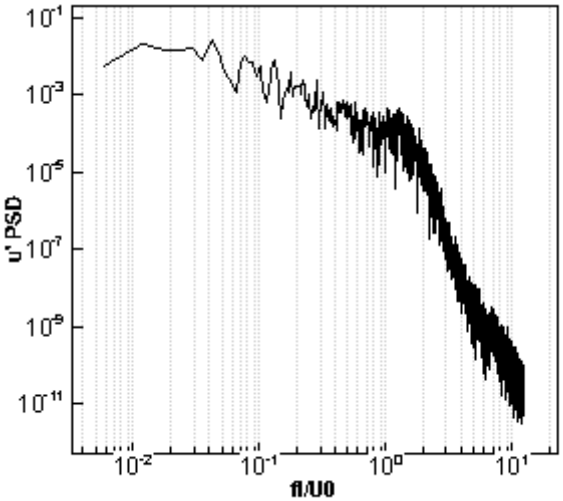

FIG. 12. Power spectrum of streamwise velocity fluctuation *u'* at *x/l* = 0.085 and *y/l* = 0.023 (ETL-case)

The bypass transition scenario proposed above for the ETL-case can be further confirmed by studying the flow structures visualized using isosurfaces of the Q-criterion (as shown in Figure 13. Q-criterion is one of the most effevtive means to visualize flow structures and is defined as follows:

$$Q = \frac{1}{2}(\Omega_{ij}\Omega_{ij} - S_{ij}S_{ij}), \quad \Omega_{ij} = \frac{1}{2}(\frac{\partial u_i}{\partial x_j} - \frac{\partial u_j}{\partial x_i}), \quad S_{ij} = \frac{1}{2}(\frac{\partial u_i}{\partial x_j} + \frac{\partial u_j}{\partial x_i})$$

For the LTL-case the spanwise oriented quasi-2D KH rolls are clearly visible at the early stage of the bubble and then become distorted/deformed due to three-dimensional motion setting in as a result of a possible secondary instability. A kind of 3D structures similar to the so called hairpin vortices form further downstream and eventually breakdown to turbulence at about or just after the reattachment. However, for the ETL-case those spanwise oriented quasi-2D KH rolls are not visible anymore and spanwise irregularity appears at the early stage of the bubble in the separated shear layer leading to the formation 3D hairpin like structures, bypassing the stage where the quasi-2D KH rolls exist, leading to a much earlier breakdown to turbulenece compared against the LTL-case.

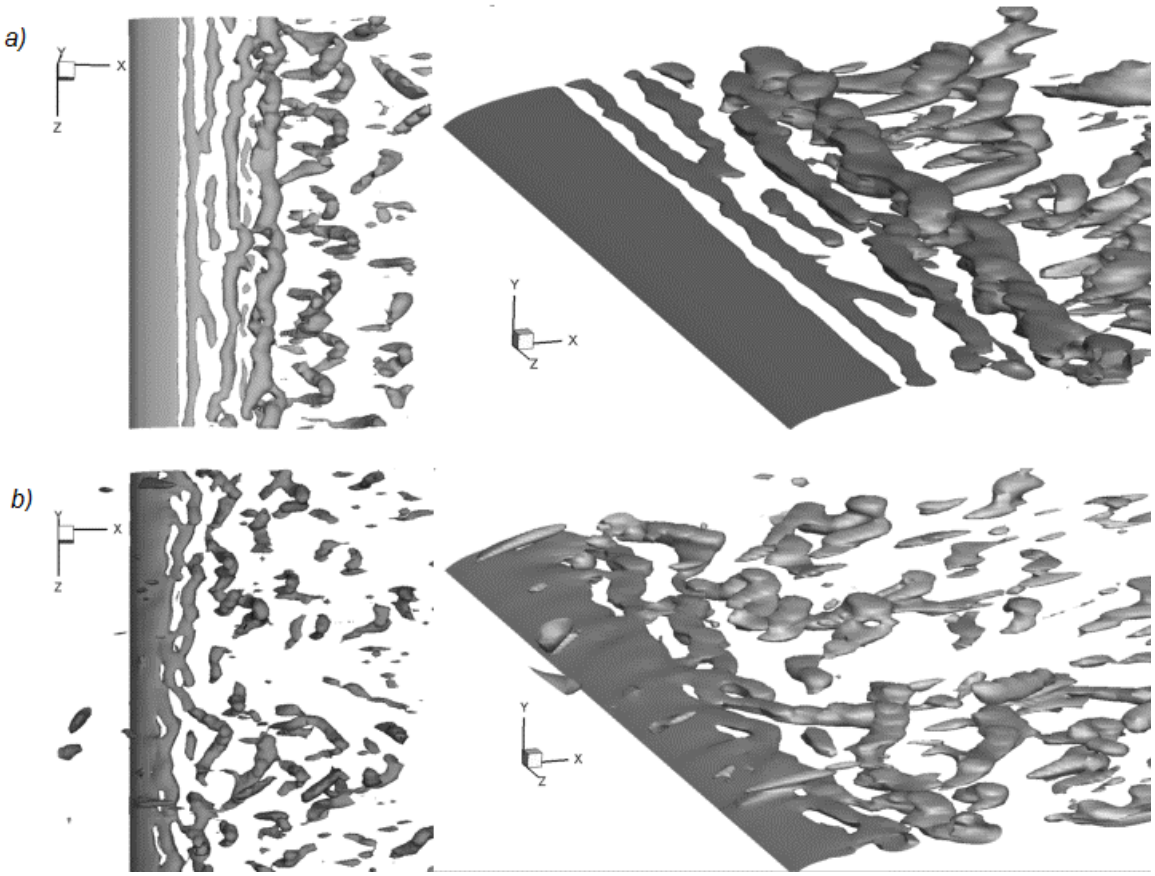

FIG. 13. Top and perspective views of the Q-criterion isosurfaces;
(a) LTL-case, (b) ETL-case

V. CONCLUSION

LES study of a transitional separated boundary layer over a flat plate with a semi-circular leading edge at two free-stream turbulence levels (<0.2 % and 5.6 % at leading edge) has been presented. The predicted mean quantities for both cases compare well with the experimental data and the entire transition process leading to breakdown to turbulence has been elucidated and visualized using the LES data for both cases.

For the LTL-case the free shear layer formed in the separation bubble is inviscidly unstable via the Kelvin-Helmholtz instability mechanism, consistent with many previous studies. However, for the ETL-case (5.6% FST level) the instability analysis shows that the criterion for the KH instability to occur is not satisfied anymore. There is already

disturbances in the attached thin boundary layer before separation and the disturbances grow very rapidly immediately after separation, leading to very rapid transition. This is further confirmed by visualizing the transition process using isosurfaces of the Q-criterion which shows that the transition process is quite different for the ETL-case compared against the LTL-case. The early stage where the KH instability occurs in the LTL-case is bypassed in the ETL-case, similar to the "bypass transition" process in attached boundary layers where TS instability stage is bypassed. It can be concluded that for the separated boundary layer flow in the present study a kind of "bypass transition" occurs under 5.6% FST level and the 2D primary instability of the free shear layer via the Kelvin-Helmholtz instability mechanism observed at lower free-stream disturbances is bypassed.

REFERENCES

[1]P.R. Spalart and M.K.H. Strelets, "Mechanisms of transition and heat transfer in a separation bubble", J. Fluid Mech. **403**, 329 (2000).

[2]Z. Yang and P.R. Voke, "Large-eddy simulation of boundary layer separation and transition at a change of surface curvature", J. Fluid Mech. **439**, 305 (2001).

[3]I.E. Abdalla and Z. Yang. "Numerical study of the instability mechanism in transitional separating-reattaching flow", International Journal of Heat and Fluid Flow **25**, 593 (2004).

[4]I.E. Abdalla and Z. Yang, "Effects of free-stream turbulence on large-scale coherent structures of separated boundary layer transition", Int. J. Numer. Meth. Fluid **49**, 331 (2005).

[5]B.R. McAuliffe and M.I. Yaras, "Transition Mechanisms in Separation Bubbles Under Low- and Elevated-Freestream Turbulence", ASME J. Turbomach. **132**, 011004 (2010).

[6]S. Burgmann, J. Dannemann and W. Schroder, "Time-resolved and volumetric PIV measurements of a transitional separation bubble on an SD7003 airfoil", Exp Fluids **44**, 609 (2008).

[7]B.R. McAuliffe and M.I. Yaras, "Passive manipulation of separation-bubble transition using surface modifications", Journal of Fluids Engineering **131**(2), 021201 (2009).

[8]F. Satta, D. Simoni, M. Ubaldi, P. Zunino, and F. Bertini, "Experimental investigation of separation and transition processes on a high- lift low-pressure turbine profile under steady and unsteady inflow at low Reynolds number", Journal of Thermal Science **19**, 26 (2010).

[9]J. Dahnert, C. Lyko, and D. Peitsch, "Transition mechanisms in laminar separated flow under Simulated low pressure turbine aerofoil conditions", Journal of Turbomachinery **135**, 011007: 1 (2012).

[10]R. Hillier and N.J. Cherry, "The effect of stream turbulence on separation bubble", Journal of Wind Engineering and Industrial Aerodynamics **8**, 49 (1981).

[11]M. Kalter and H.H. Fernholz, "The reduction and elimination of a closed separation region by free-stream turbulence", J. Fluid Mech. **446**, 271 (2001).

[12]I.P. Castro and A. Haque, "The structure of a shear layer bounding a separation region. Part 2. Effects of free-stream turbulence", J. Fluid Mech. **192**, 577 (1988).

[13]R.J. Volino and D.G. Bohl, "Separated Flow Transition Mechanism and Prediction with High and Low Free stream Turbulence Under Low Pressure Turbine Conditions", ASME GT2004-53360 (2004).

[14]R.J. Volino, "Separated Flow Transition Under Simulated Low- Pressure Turbine Airfoil Conditions: Part 2-Turbulence Spectra", ASME J. Turbomach. **124**, 656 (2002).

[15]Z. Yang and I.E. Abdalla, "Effects of free-stream turbulence on a transitional separated-reattached flow over a flat plate with a sharp leading edge", Int. J. Heat Fluid Flow **30**, 1026 (2009).

[16]C. Pokora, W. McMullan, G. Page, and J. McGuirk, "Influence of a Numerical Boundary Layer Trips on Spatio- Temporal Correlations within LES of a Subsonic Jet", AIAA Paper No. 2011-2920, 2011.

[17]M. Germano, M. Piomelli, P. Moin, and W.H. Cabot, "A dynamic subgrid-scale eddy viscosity model", Phys. Fluids **A(3)**, 1760 (1991).

[18]D.K. Lilly, "A proposed modification of the Germano subgrid-scale closure method", Phys. Fluid **A(4)**, 633 (1992).

[19]T.F. Miller and F.W. Schmidt, "Use of a pressure-weighted interpolation method for the solution of the incompressible Navier-Stokes equations on a non-staggered grid system", Numerical Heat Transfer **14**, 213(1988).

[20]M. Peric, R. Kessler, and G. Scheuerer, "Comparison of finite-volume numerical methods with staggered and collocated grids", Computer & Fluids **16**, 389(1988).

[21]M.C. Melaaen, “Calculation of fluid flows with staggered and non-staggered curvilinear non-orthogonal grids – a comparison”, Numerical Heat Transfer **21**, 1 (1992).

[22]Y. Zang, R.L. Street, and J.R. Koseff, “A non-staggered grid, fraction step method for time-dependent incompressible Navier-Stokes equations in curvilinear coordinates”, Journal of Computational Physics **114**, 18 (1994).

[23]P. Schlatter, L. Brandt, H. C. de Lange, and Dan S. Henningson, “On streak breakdown in bypass transition”, Phys. Fluids **20**, 101505 (2008).

[24]J. H. Watmuff, D. A. Pook, T. Sayadi, and X. Wu, “Fundamental physical processes associated with bypass transition”, Center for Turbulence Research, Proceedings of the Summer Program 2010, 97 (2010).

[25]L. Brandt, Dan S. Henningson, “Direct Numerical Simulations of Streak Breakdown in Boundary Layers”, *Direct and Large-Eddy Simulation V*, ERCOFTAC Series **9**, 175 (2004).

[26]S. Chanderasekhar, *Hydrodynamic and Hydromagnetic Stability* (Clarendon, 1961).